Molecular and Ionic Hydrogen Bond Formation in Fluorous Solvents

ARTICLE *in* THE JOURNAL OF PHYSICAL CHEMISTRY B · FEBRUARY 2009

Impact Factor: 3.3 · DOI: 10.1021/jp8084155 · Source: PubMed

2 AUTHORS:

Kristi Kauffman
PPG Industries
9 PUBLICATIONS **74** CITATIONS
SEE PROFILE

Stephen Gregory Weber
University of Pittsburgh
233 PUBLICATIONS **3,555** CITATIONS
SEE PROFILE

THE JOURNAL OF PHYSICAL CHEMISTRY B

Article

Molecular and Ionic Hydrogen Bond Formation in Fluorous Solvents

Kristi L. O'Neal, and Stephen G. Weber

J. Phys. Chem. B, **2009**, 113 (1), 149-158• DOI: 10.1021/jp8084155 • Publication Date (Web): 16 December 2008

Molecular and Ionic Hydrogen Bond Formation in Fluorous Solvents

Kristi L. O'Neal and Stephen G. Weber*

Department of Chemistry, University of Pittsburgh, Pittsburgh, Pennsylvania 15260-3900

Received: September 22, 2008; Revised Manuscript Received: November 3, 2008

There are only a few studies of noncovalent association in fluorous solvents and even fewer that are quantitative. A full understanding, particularly of stoichiometry and binding strength of noncovalent interactions in fluorous solvents could be very useful in improved molecular-receptor-based extractions, advancements in sensor technologies, crystal engineering, and supramolecular chemistry. This work investigates hydrogen bonding between heterocyclic bases and a perfluoropolyether with a terminal carboxylic acid group (Krytox 157FSH (**1**)), chiefly in FC-72 (a mixture of perfluorohexanes). In particular, we were interested in whether or not proton transfer occurs, and if so, under what conditions in H-bonded complexes. Continuous variations experiments show that in FC-72 weaker bases (pyrazine, pyrimidine, and quinazoline) form 1:1 complexes with **1**, whereas stronger bases (quinoline, pyridine, and isoquinoline) form 1:3 complexes. Ultraviolet and infrared spectral signatures reveal that the 1:1 complexes are molecular (B·HA) whereas the 1:3 complexes are ionic ($BH^+ \cdot A^-$ HAHA). Infrared spectra of 1:3 ionic complexes are discussed in detail. Literature and experimental data on complexes between N-heterocyclic bases and carboxylic acids in a range of solvents are compiled to compare solvent effects on proton transfer. Polar solvents support ionic hydrogen bonds at a 1:1 mol ratio. In nonpolar organic solvents, ionic hydrogen bonds are only observed in complexes with 1:2 (base/acid) stoichiometries. In fluorous solvents, a larger excess of acid, 1:3, is necessary to facilitate proton transfer in hydrogen bonds between carboxylic acids and the bases studied.

1. Introduction

Noncovalent interactions facilitate a remarkable range of applications of chemistry.[1−3] Artificial molecular receptors have been used to enhance selectivity and to minimize solvent consumption for the extraction of a wide variety of target molecules.[4−9] Selectivity is high if noncovalent intermolecular interactions between receptor and target dominate the standard-state free energy change for the extraction process. These interactions become less important in competitive solvents;[10] thus, a matrix that is a poor solvent will provide a more selective environment for molecular recognition interactions.[11,12]

Poorly solvating, highly nonpolar fluorous liquids are practically immiscible with both aqueous and organic phases[13] and, with the exception of some small gases, nonfluorous solutes are, in general, virtually insoluble in them. Thus, fluorous liquids have become useful for purification and reaction cleanup[13−15] by reducing the unintentional extraction of interfering species. Fluorous separations become possible by covalent labeling of a product precursor or catalyst with a fluorous tag for easy separation of the labeled entities through extraction with fluorous liquids. However, noncovalent approaches based on noncovalent complex formation are more desirable because they are more straightforward and have applications where selective, covalent labeling of a target molecule is impossible, impractical, or undesirable. Molecular recognition in combination with fluorous matrices should improve the selectivity of molecular extractions by reducing the number and amount of interfering species extracted and increasing the strength of the substrate−receptor interactions by eliminating solute−solvent competition.[13,14,16] Perfluoroalkane-based amine[17] and phosphine[18] ligands have been shown to support metals in fluorous liquids. Pyridyl tags can be used in conjunction with perfluorocarboxylate-supported copper to extract porphyrins and fullerenes.[19,20] Boswell et al.[21−23] have used fluorous liquids to provide a medium for more stable ion−ionophore complexes, thereby creating exceptionally selective sensor membranes. We have recently reported that a carboxylic acid-terminated poly hexafluoropropylene oxide, Krytox 157FSH (**1**), significantly enhances the extraction of pyridine (100-fold with excess **1** as compared to **1**-free) and substituted pyridines from chloroform into a mixture of perfluorohexanes (FC-72).[12]

$$\text{Krytox 157FSH}/CF_3 - CF_2 - CF_2 - O - [CF(CF_3)CF_2 - O-]_nCOOH_n \cong 29$$

1 is a suitable molecular receptor for the fluorous phase because the ether oxygens are not basic[21] and it is soluble only in highly fluorinated solvents.[22] We have previously found that **1** extracts pyridine into the fluorous solvent FC-72. A 1:3 (pyridinium/$\mathbf{1}^-$) H-bonded complex is formed. We estimated the free energy of formation of the complex from a free acid, pyridine, and a carboxylic acid dimer to be −39 kJ mol^{-1}; thus reporting the first hydrogen bond strength in a fluorous environment.[12]

Complexes between pyridine and HF also form molecular and ionic hydrogen bonds depending on the stoichiometry. In the crystalline state, 1:1 complexes exhibit molecular hydrogen bonds (N−HF) whereas higher order 1:2 and 1:3 (pyridine/HF) complexes contain ionic hydrogen bonds.[23] Low-temperature NMR studies of pyridine−acetic acid complexes in a 2:1 mixture of $CDClF_2$ and CDF_3 show that 1:1, 1:2, and 1:3 complexes are formed.[24] The hydrogen bond is strengthened and the proton is transferred from acetic acid to pyridine as the order of the complex increases.

It is known that the pyridine nitrogen interacts strongly with carboxylic acids. Both hydrogen-bonded molecular complexes

* To whom correspondence should be addressed. E-mail: sweber@pitt.edu.

10.1021/jp8084155 CCC: $40.75
Published on Web 12/16/2008

(N—HO) and ionic complexes (NH^+—O^-) in which the proton is transferred are possible. There has been a great deal of interest in the degree of proton transfer in acid—pyridine complexes under various conditions; thus, relevant UV/vis, IR, and NMR spectroscopic signals of pyridines in the presence of acids are well-documented.[24−35] A study of the state of proton transfer in hydrogen-bonded pyridine complexes shows a gradual shift of the proton toward the nitrogen atom with increasing H-bond donor acidity and, for a given complex, the N—H distance falls with increasing solvent dielectric constant.[29] Changes in the IR spectrum show that in going from the gas phase to the condensed phase, as well as upon increasing solvent polarity, the hydrogen bond in a pyridine—acetic acid complex is strengthened and the proton is transferred to the nitrogen atom.[32] The body of work on carboxylic acid—pyridine complexes agrees that polar environments strengthen hydrogen bonds and support proton transfer through ordering and polarization of the solvent in the vicinity of the hydrogen bond.[29,31,32,36−38] Thus the question arises, to what extent can nonpolarizable fluorous liquids support proton transfer?

It is evident from this collection of work that proton transfer is sensitive to the environment beyond the immediate configuration of the hydrogen bond. Here, we investigate the proton transfer phenomenon in fluorous matrices to gain insight into noncovalent interactions in such environments. This study is specifically aimed at providing a fundamental understanding of the influence had by fluorous solvents on the stoichiometry and binding strength of noncovalent interactions and at ultimately improving extractions through the use of artificial receptors in fluorous liquids. A better understanding of noncovalent interactions in a fluorous matrix will also have potential applications in new sensor technologies, crystal engineering, and supramolecular chemistry.

2. Experimental Section

2.1. Chemicals and Instrumentation. Pyrazine, pyrimidine, quinazoline, quinoline, isoquinoline, potassium bromide, dichloroacetic acid, and perfluorodecanoic acid (PFDA) were obtained from Aldrich (Milwaukee, WI); pyridine and cyclohexane were purchased from J.T. Baker (Phillipsburg, NJ); and benzene was obtained from EMD Chemicals Inc. (Gibbstown, NJ). Monochloroacetic acid was purchased from Mallinckrodt (St. Louis, MO), and trichloroacetic acid is from Fisher Scientific (Pittsburgh, PA). Mono-, di-, and trifluoroacetic acids were purchased from Acros (NJ). FC-72 fluororoinert electronic liquid (a mixture of perfluorohexanes) was obtained from 3M (St. Paul, MN). HFE-7100 (a mixture of perfluoro-*n*-butyl and perfluoroisobutyl methyl ether) and Krytox 157FSH (**1**) were purchased from Miller-Stephenson Chemical Co., Inc. (Danbury, CT). All the chemicals listed above were used as received. Chloroform was purchased from Fisher Scientific (Fair Lawn, NJ), dried over molecular sieves, and treated with potassium carbonate (EM Science, Cherry Hill, NJ) to neutralize any HCl that may have formed as a result of exposure to light. Note that perfluorocarboxylates are known to be environmentally persistent and should be handled accordingly. ^{19}F-NMR analysis of **1** resulted in a number-averaged molecular weight of 5150 g mol^{-1} with an average of 29 polymer repeat units. It should be noted that we previously reported[12] a number-averaged molecular weight of 5840 g mol^{-1} with 33 repeat units for Krytox 157FSH. The difference lies in variability between batches.

A Hewlett-Packard 8452A UV—visible diode array spectrophotometer was used for all the UV absorbance measurements. A quartz cell with a path length of 0.1 cm was purchased from Fisher Scientific (Pittsburgh, PA) and was used for all measurements.

A Varian Excalibur FT-IR spectrophotometer was used for all IR measurements, and all spectra were analyzed using Varian Resolutions Pro 4.2 software package. An amalgamated KBr liquid sample cell with a 1.0 mm path length and holder was purchased from International Crystal Laboratories (Garfield, NJ) and was used for liquid samples. Liquid samples were measured against a solvent background at a resolution of 2 cm^{-1} with 50 scans averaged. "Solvent-free" samples were measured against a blank background in KBr salt plates with a 0.1 mm lead spacer obtained from Wilmad (Buena, NJ) at a resolution of 2 cm^{-1} with 50 scans averaged. A titration of **1** with quinoline in FC-72 was measured at a resolution of 0.25 cm^{-1} with 500 scans averaged, smoothed using a 49-point boxcar, and baseline corrected to achieve a higher signal-to-noise ratio. All other IR spectra were smoothed using a 5-point boxcar and were baseline corrected. A Jouan A12 centrifuge was used for the solvent-free samples.

The mixed solvent method was used for slow precipitation of PFDA—quinoline crystals. A 1.0 mL portion of 5.0 mM PFDA in FC-72 was mixed with 1.0 mL of quinoline-saturated HFE-7100 in a 20 mL scintillation vial, and the mixture was placed in a mechanical shaker (in-house construction) for 10 min, followed by 10 min in the ultrasonicator bath. The solution was transferred to a small Petri dish where it was lightly covered with weighing paper and allowed to cool and evaporate slowly overnight. A 1.9 mg portion of crystalline material was then mixed with 99.0 mg of KBr in a mortar and pestle and transferred to a pellet press obtained from International Crystal Laboratories (Garfield, NJ). IR spectra of the resulting pellets were measured at a resolution of 4 cm^{-1} with 20 scans averaged.

2.2. Spectroscopy-based Determination of Stoichiometry and Formation Constants. The UV continuous variations data were obtained by creating a series of solutions from 1.00 mM base and 1.00 mM acid so that the molar sum of base and acid remained constant.[39,40] All stock solutions were placed in a Cole—Parmer (Chicago, IL) ultrasonicator bath for 10—30 min to ensure dissolution of the materials in their respective solvents. The method for normalized continuous variations plots was derived based on the general method developed by Likussar.[41] See the Supporting Information for the derivation. The UV titration data were obtained by titrating 0.50 mL of 2.00 mM base with 5.00 mM acid and diluting to a constant volume of 1.00 mL with a final base concentration of 1.00 mM. All samples were shaken for 10 min on a mechanical shaker (in-house construction) to ensure homogeneity and then allowed to rest for 10 min before measurements were made. All absorbance values were measured under ambient conditions (22.0 ± 1 °C) and were baseline corrected. The UV difference absorbance as discussed by Valenta[4] is related to the amount of acid—base complex present in solution and was measured as a function of the fraction acid for continuous variations experiments and acid/base ratio for titrations. Specfit/32[42] software package distributed by Spectrum Software Associates (Marlborough, MA) was used for two separate treatments of spectroscopic data. In one, a nonlinear regression approach estimates binding constants based on a set of spectra and assumed complex stoichiometries. In the other, there are no chemical assumptions. Evolving factor analysis (EFA) of the experimental and difference spectra lead directly to the number of individual spectra (i.e., chemical species) contributing to the observed set of spectra.

IR solution titration data were obtained by titrating 0.25 mL of 10.00 mM **1** in FC-72 with 10.00 mM base and diluting to

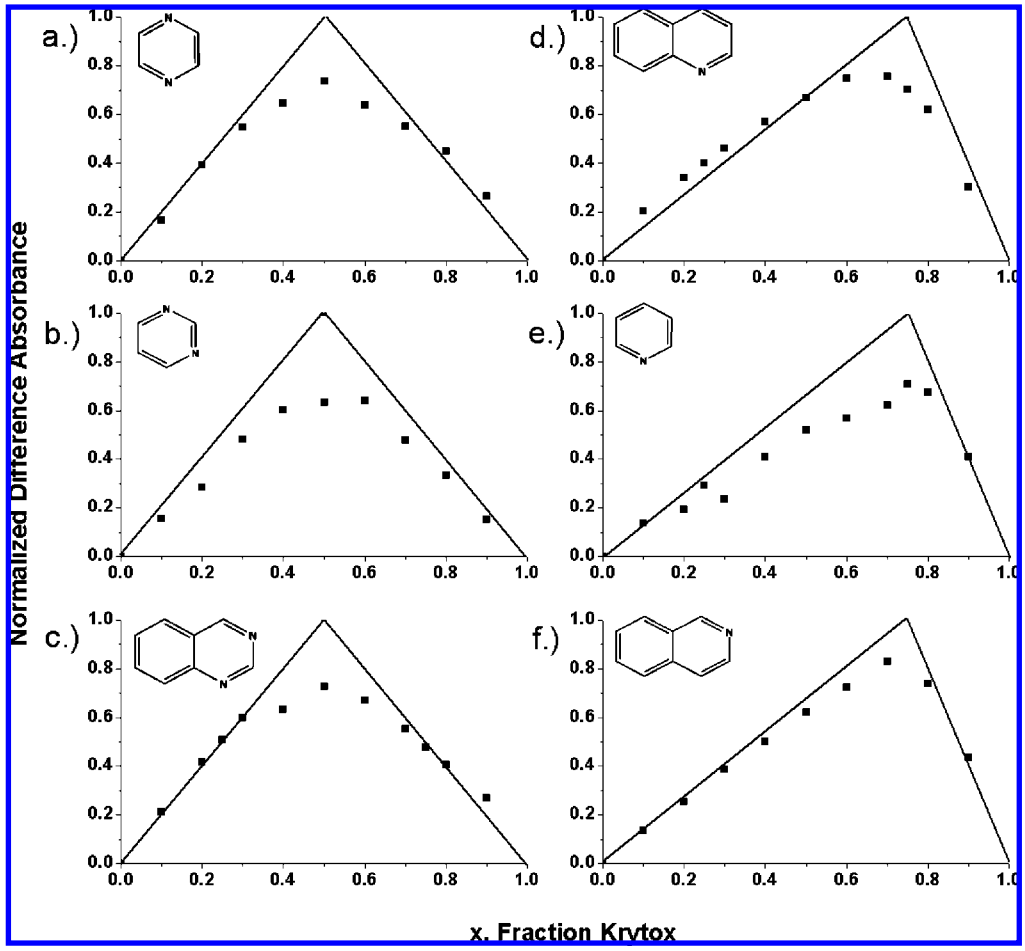

Figure 1. Representative normalized continuous variations plots for (a) pyrazine, (b) pyrimidine, (c) quinazoline, (d) quinoline, (e) pyridine, and (f) isoquinoline with **1** in FC-72 shown as a function of sample composition. The data points represent absorbances normalized relative to a solution containing a definite excess of acid in which all base is associated with acid. Lines correspond to the expected difference absorbance if the complexation reaction goes to completion at each concentration ratio.

a constant volume of 0.50 mL, resulting in 5.00 mM final **1** concentration in each sample. For solvent-free IR titrations, precisely weighed aliquots of **1** were added to 1.0 μL neat base, stirred, and centrifuged for 10 min.

3. Results and Discussion

No single experimental result tells the entire story. For the most part, we have relied on electronic absorption spectra (actually, difference spectra, as there are typically no new bands associated with the complexes formed) for stoichiometry and estimates of formation constants. For some complexes, there is literature on electronic spectroscopic changes accompanying proton transfer ($BH^+—A^-$, where B and HA are the initial base and acids) versus those in which it has not occurred (B—HA). Although useful, those changes are often subtle, so infrared spectra are then used for distinguishing complexes in which proton transfer has occurred.

3.1. Stoichiometry and Formation Constant. We used the method of continuous variations[39,41] (see Supporting Information) based on difference absorbance spectra to determine the stoichiometric ratio in complexes of **1** with pyridine, quinoline, isoquinoline, quinazoline, pyrazine, and pyrimidine in FC-72. These substrates were chosen because they demonstrated some solubility in **1**-free FC-72, allowing separate solutions of receptor and substrate to be prepared. However, despite the apparent solubility in FC-72, there is no measurable partitioning of any of the six bases listed above from 1.0 mM chloroform solutions into FC-72 at room temperature with a phase ratio of 1.0.

The continuous variations plots (Figure 1) reveal 1:1 stoichiometries for **1** complexes with pyrazine, pyrimidine, and quinazoline and 1:3 (base:acid) stoichiometries with quinoline, pyridine, and isoquinoline in FC-72. From the continuous variations data, we applied the normalized absorbance method[41,43] to determine the formation constant (K_f) and hence the free energy of formation, ΔG_f° (1), of complexes with **1**, where R is the gas constant and T is temperature.

$$\Delta G_f^\circ = -RT \ln(K_f) \quad (1)$$

In this method, absorbances are normalized to the absorbance obtained from a solution containing excess **1**. In such a solution there is effectively no free base, thus the measured absorbance represents only complex (see the Supporting Information for derivation). The lines in Figure 1 correspond to the expected difference absorbance if the complexation reaction goes to completion at each concentration ratio. Hypochromic effects from base self-association were not observed in the experimental concentration range (0.1−1.0 mM). Nonetheless, in the continuous variations plot of quinoline (Figure 1d) data points for $x <$ 0.5 fall above the "expected" lines for complete complexation.

TABLE 1: Stoichiometry, Formation Constant, and Free Energy of Formation for a Series of Pyridine-like Bases with 1 in FC-72 Determined by the Method of Continuous Variations, Titrations, and Specfit Global Fitting

substrate	pK_a[a]	stoichiometry base/**1**	K_f (M^{-1})	complex ΔG_f° (kJ/mol)	ΔG_f° SEM[b] (kJ/mol)	N[c]
pyrazine	0.7	1:1	$(1.5 \pm 0.2) \times 10^4$	−24	0.3	7
pyrimidine	1.2	1:1	$(1.6 \pm 0.2) \times 10^3$	−23	0.3	6
quinazoline	3.4	1:1	$(8.8 \pm 1.7) \times 10^4$	−22	0.3	4
quinoline	4.9	1:3	$(2.4 \pm 0.3) \times 10^{13}$	−73	0.8	8
pyridine	5.2	1:3	$(3.6 \pm 0.5) \times 10^{11}$	−65	0.8	6
isoquinoline	5.4	1:3	$(2.8 \pm 0.5) \times 10^8$	−47	0.7	4

[a] Aqueous pK_a values for the conjugate acid. [b] ΔG_f° standard errors of the mean (SEM) were determined from a ΔG_f° pooled relative standard deviation for the method of 3.2%. [c] Number of determinations.

This is explained by the sequential formation of 1:1, 1:2, and 1:3 quinoline/**1** complexes with increasing **1** and will be discussed in the following section. Continuous variations experiments in which one of the "reagents" was taken to be the dimer, $\mathbf{1}_2$, were performed to rule out the possibility of a dominant species with 1:2 stoichiometry for this particular complex (Figure S1, Supporting Information). The results confirmed the 1:3 complex as the predominant complex.

Table 1 shows data for the six bases listed in the order (low to high) of the aqueous pK_a of their conjugate acids. Formation constants determined several ways from multiple experiments agree reasonably well. To verify the accuracy of the formation constants and to validate the normalized continuous variations method, regression analysis (Specfit[42]) was applied to both continuous variations and titration data for each base. Formation constants are calculated for complexes of user-defined stoichiometries. Incorrect "guesses" at what complexes are present are indicated by very large errors in the estimated binding constants. Formation constants determined from fitting the data to an assumed set of chemical equilibria were in good overall agreement with those determined from the normalized continuous variations method. A straightforward 1:1 model was used for pyrazine, pyrimidine, and quinazoline complexes with **1**, whereas a more complex model including 1:1, 1:2, and 1:3 (base/acid) complexes was employed for quinoline, pyridine, and isoquinoline. A simple model specifying the formation of a 1:3 complex alone was not sufficient to explain the data for any of these three bases. Formation constants (K_f) and free energies of formation (ΔG_f°) reported in Table 1 are mean values from normalized continuous variations and regression analysis on titrations and continuous variations data. These do not depend monotonically on the pK_a values. It becomes clear that the stronger bases demonstrate a 1:3 (base/acid) stoichiometry whereas the weaker bases show a 1:1 stoichiometry.

3.2. Molecular vs Ionic Complex Formation. ***3.2.1. Ultraviolet Spectra.*** Spectra and titration curves for constant-volume titrations of pyrazine, pyrimidine, quinazoline, quinoline, pyridine, and isoquinoline with **1** in FC-72 are shown in the Supporting Information (Figures S2−S15). Let us first discuss the 1:1 complexes of **1** with pyrimidine, pyrazine, and quinazoline. In FC-72, the spectrum of pyrimidine (Figure S4) has two systems of bands, $\pi \rightarrow \pi^*$ bands near 240 nm and $n \rightarrow \pi^*$ bands near 300 nm. In a titration of pyrimidine with **1** in FC-72 (Figures S2−S3), the absorption maximum associated with the $n \rightarrow \pi^*$ transition (300 nm) persists but shifts to shorter wavelengths (273 nm) with increasing [**1**]. In neutral or basic aqueous solutions, the $n \rightarrow \pi^*$ bands are at 270 nm.[44] In acidic aqueous solutions where pyrimidine is protonated, the $n \rightarrow \pi^*$ band is not observed.[44] Thus, electronic spectra are consistent with a 1:1 complex that is comprised of **1** hydrogen-bonded to pyrimidine with no proton transfer. Spectra of pyrazine show similar behavior (Figures S4−S5). In neutral and basic aqueous solutions[45] as well as in FC-72 solutions with **1**, the spectrum of pyrazine has a $\pi \rightarrow \pi^*$ band near 260 nm and an $n \rightarrow \pi^*$ band between 300−325 nm. The spectrum of protonated pyrazine in acidic aqueuous solutions shows no $n \rightarrow \pi^*$ band;[45] thus, the observation of this band in FC-72 solutions with **1** is evidence for the molecular complex. The spectrum of quinazoline changes markedly upon protonation,[46] yet a titration of quinazoline with **1** (Figures S6−S7) did not produce substantial changes. Only a small hypsochromic shift in the $\pi \rightarrow \pi^*$ transition band and a loss in vibronic structure of the $n \rightarrow \pi^*$ band were observed. This is evidence that the complex of quinazoline with **1** is hydrogen-bonded with no proton transfer.

The 1:3 complexes formed by pyridine, isoquinoline, and quinoline with **1** in FC-72 show different behavior. The spectrum of pyridine in FC-72 (Figures S8−S9) shows three distinguishable bands at 249, 255, and 261 nm, similar to the spectrum of pyridine in neutral or basic aqueous solutions that show maxima at 250, 256, and 261 nm.[47] After addition of **1** to a solution of pyridine in FC-72, the maximum remains at 255 nm, whereas the other component bands become shoulders. The same behavior was observed with pyridine in acidic aqueous solutions,[47] indicating that proton transfer from **1** to pyridine occurs in FC-72. We have previously reported a detailed study on this complex.[12]

The electronic absorption spectrum of isoquinoline in FC-72 (Figure S10) has a $\pi \rightarrow \pi^*$ band at 262 and an $n \rightarrow \pi^*$ band at 315 nm that is rich in vibronic structure. A constant-volume titration of isoquinoline with **1** in FC-72 (Figures S10−S12) reveals two new $n \rightarrow \pi^*$ bands at 320 and 327 nm with addition of **1**. There is a complete loss of vibronic structure in the $n \rightarrow \pi^*$ band at 3:1 and greater excess of **1**. A similar loss of vibronic structure has been observed for a 1:2 isoquinoline:trifluoroacetic acid complex in acetonitrile in which the acid has transferred a proton to isoquinoline.[48] For 1:1 molecular isoquinoline−trifluoroacetic acid complexes with no proton transfer in octane and carbon tetrachloride, the vibronic structure is intact and no new peaks appear.[48] Titration curves in FC-72 (Figure S11) show the formation of two different complexes with 1:2 and 1:3 (isoquinoline/**1**) stoichiometries. Meanwhile, the position of the $\pi \rightarrow \pi^*$ band gradually shifts from 262 to 271 nm as **1** is added but remains at 271 nm at 3:1 excess of **1** and greater (see Figure S12). Thus, the data indicate that proton transfer occurs in FC-72 as the excess of **1** to isoquinoline reaches 3 and beyond.

The electronic absorption difference spectra resulting from a constant-volume titration of quinoline with **1** in FC-72 are shown in Figure 2. Original absorbance spectra are shown in the Supporting Information (Figure S13). A close look at the difference absorbance from 220−240 nm shows a peak at 230 nm and a shoulder at 232 nm that appears at 1:2 (quinoline/**1**) mole ratios, neither of which are present in the spectrum of free quinoline. Figure 3 shows the intensity of these peaks as a function of mole ratio. The difference in the shape of the curves

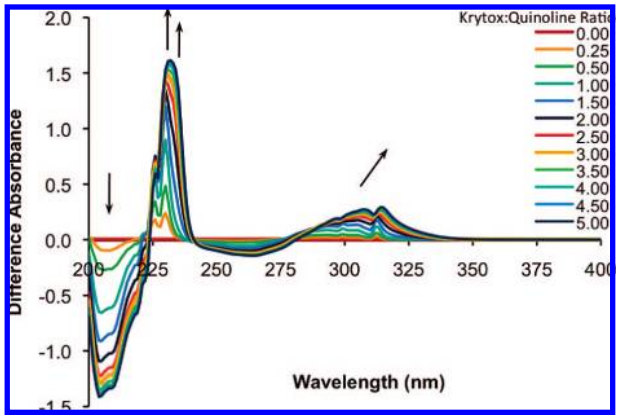

Figure 2. Difference absorbance spectra resulting from a constant-volume titration of 1.0 mM quinoline with **1** in FC-72. Arrows indicate increasing [**1**].

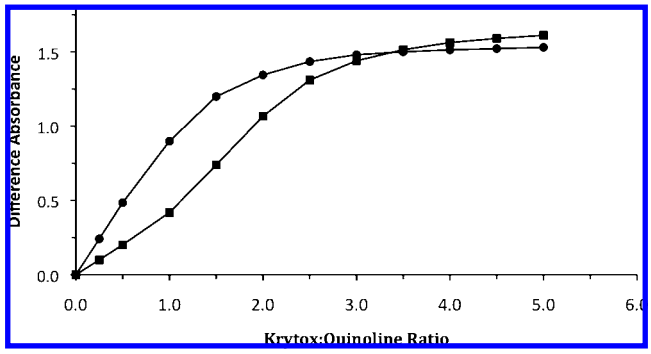

Figure 3. Titration curve at (●) 230 and (■) 232 nm of constant 1.0 mM quinoline with **1** in FC-72.

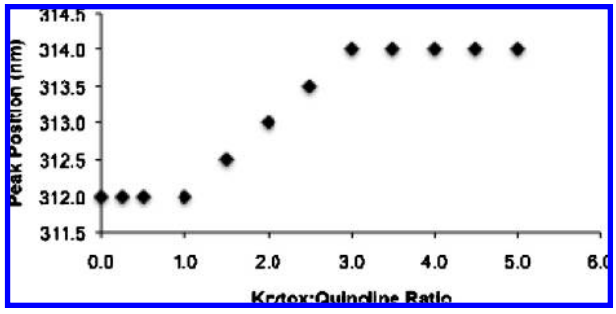

Figure 4. Peak position as a function of **1**/quinoline mole ratio in the constant-volume titration of 1.0 mM quinoline with **1** in FC-72.

at the two wavelengths is further indication of the presence of more than one complex. From the titration curve at 230 nm (Figure 3), it is clear that there is a 1:2 hydrogen-bonded complex, although the titration curve at 232 nm suggests a 1:3 complex. A look at the remainder of the electronic spectrum reveals a sharp peak at 312 that exhibits a bathochromic shift with increasing [**1**]. Such a shift often indicates changes in the polarity of the environment or a strengthening of the hydrogen bond.[49] The position of this peak as a function of mole ratio (Figure 4) shows that there is a transition between 1:1 and 1:3 (quinoline/**1**) mole ratios.

3.2.2. Factor Analysis. Factor analysis can be used to simplify the analysis of mixtures based on correlations among the spectra from solutions containing the same compounds but with various compositions. Singular value decomposition (SVD) produces linearly independent eigenvectors with all the spectroscopic information plus the noise contained in a data matrix (set of spectra). The number of significant (i.e., not due to noise)

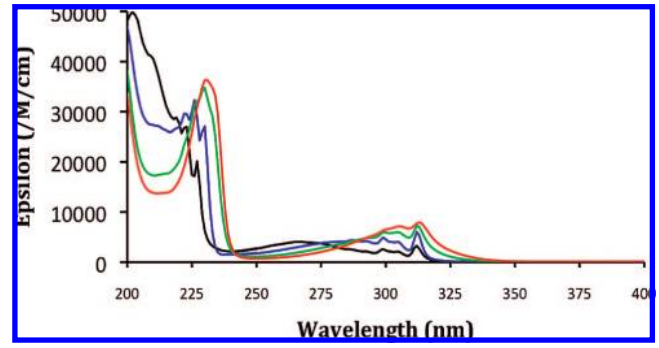

Figure 5. EFA predicted spectra of free quinoline (black), a 1:1 (blue), 1:2 (green), and 1:3 (red) quinoline/**1** complex. The spectral regions 200−250 and 250−400 nm were calculated independently yet line up with excellent agreement.

eigenvectors is equal to the number of chemical species contributing to the observed spectroscopic changes.[50] The program Specfit[42] carries out this sort of analysis, allowing for the determination of the number of chemical entities contributing to the observed spectra. The program can also be used to estimate how the contributions of the chemical entities change with conditions, for example, as concentrations are changed. The latter estimation is called "model-free evolving factor analysis (EFA) applied following SVD". It is quite successful at determining the concentration profiles and component spectra from a series of spectra. The term "model-free" means that the user does not specify how many complexes are present, stoichiometries, etc. The user only provides a set of spectra and initial component concentrations. As described above, a regression analysis based on assumed complex stoichiometries can also be carried out. The two analyses should show the same result.

We applied EFA to two regions of the spectrum independently, one below 250 nm and one above. In both spectroscopic regions, four factors (i.e., optically absorbing chemical species) were sufficient to explain the data. The predicted spectra corresponding to these chemical species are shown in Figure 5. These spectra account for >99.9% of the variance in the data set. It is noteworthy that the spectra were analyzed in two sections (<250 nm and ≥250 nm). The two sets of predicted spectra, one from <250 nm and the other from ≥250 nm, fit together seamlessly in Figure 5. To perform a fit to the data, the complex stoichiometries have to be identified. From the factor analysis, we know that we must identify four chemical species. These are base, and complexes with stoichiometry 1:1, 1:2, and 1:3. The program does not give a spectrum for free acid because it is nonabsorbing in the wavelength range studied. The program gives best-fit concentration profiles and equilibrium constants for each reaction. Concentration profiles from the regression analysis are in good agreement with concentration profiles resulting from the model-free EFA approach as seen in Figure 6. The fit shows that the concentration of a 1:1 hydrogen-bonded (quinoline/**1**) complex increases as the amount of free quinoline decreases until all free quinoline has been consumed. A 1:2 (quinoline/**1**) hydrogen-bonded complex begins to appear and reaches a maximum, whereas the concentration of the 1:1 complex decreases as it is converted to 1:2. A 1:3 complex is dominant beyond a 3:1 excess of **1** and coexists with excess **1**-dimer (nonabsorbing from 200−400 nm). The concentration profiles determined independently from the two spectroscopic regions are in good agreement. The EFA predicted spectra for each absorbing species, free quinoline, 1:1 and 1:2 (quinoline:**1**) molecular complexes, and a 1:3 ionic complex, are shown

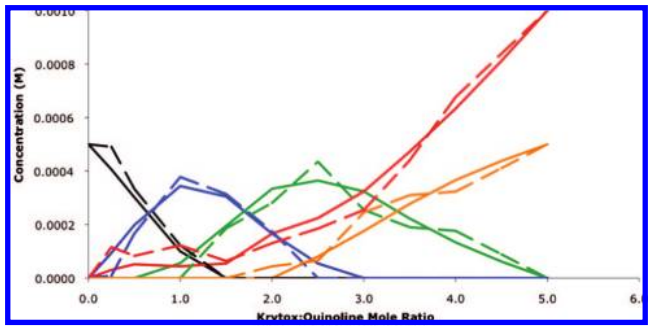

Figure 6. Overlay of concentration profiles from model-free EFA of two separate regions in the ultraviolet spectrum; (—) 200−250 nm and 250−400 nm (---) in the titration of quinoline with **1** in FC-72 for free quinoline (black), a 1:1 (blue), 1:2 (green), and 1:3 (orange) quinoline/**1** complex, and free **1** (red), respectively.

TABLE 2: Formation Constant and Free Energy of Formation for 1:1 Base/1 Complexes in FC-72 Determined by Regression Analysis of Continuous Variations and Titrations Data

substrate	pK_a	K_f (M^{-1})	1:1 complex ΔG_f° (kJ/mol)	N
quinoline	4.9	1.8×10^8	−34	4
pyridine	5.2	7.8×10^3	−22	3
isoquinoline	5.4	5.7×10^2	−16	2

in Figure 5 and correspond to the sequential complex formation shown in the concentration profiles.

Table 2 lists the formation constants and free energies for 1:1 complexes of quinoline, pyridine, and isoquinoline with **1** in FC-72 determined through the regression analysis. Of the bases listed, quinoline forms the most stable 1:1 complex. It was mentioned above that the left-hand portion of Figure 1d shows experimental difference absorbances greater than expected for complete 1:3 complex formation. The large formation constant for the 1:1 complex explains this. For comparison, concentration profiles resulting from a regression as well as those from the EFA approach for an isoquinoline-**1** complex in FC-72 are shown in the Supporting Information (Figure S15). Regression analysis and model-free EFA also confirms the sequential formation of 1:1, 1:2, and 1:3 complexes between isoquinoline and **1**.

3.2.3. Infrared Spectra. IR titrations of **1** with each base were performed. Representative spectra of the 1:1 complexes with **1**, pyrazine, pyrimidine, and quinazoline, as well as those of 1:3 complexes, quinoline, pyridine, and isoquinoline, are shown in Figure 7, panels a−c and d−f, respectively. Protonation of the heterocyclic nitrogen changes the vibrational spectrum of the complex. The C═O group of free and hydrogen-bonded carboxylic acids produces a strong band in the 1800−1700 cm^{-1} region, whereas the COO^- group of an ionized carboxylate salt exhibits a strong band between 1700 and 1550 cm^{-1}.[49] For each of the bases that formed 1:1 complexes with **1**—pyrazine, pyrimidine, and quinazoline—the carbonyl band broadened upon complex formation (Figures 7a−c) as expected for hydrogen-bond formation. On the other hand, the IR spectra of the bases that formed 1:3 complexes with **1**—quinoline, pyridine, and isoquinoline—revealed a new band centered around 1650 cm^{-1} (Figure 7d−f) that can be attributed to a carboxylate vibration. This is in agreement with the postulation from the electronic spectra, that the 1:1 complexes with **1** in FC-72 are molecular whereas the 1:3 complexes are ionic.

To gain a better understanding of proton transfer interactions in such a nonpolar environment, the remainder of this section will be focused on the IR spectra of 1:3 complexes of quinoline, isoquinoline, and pyridine with **1**. In addition, a few comments on the experiments and display of data are in order. We have learned that the information derived from IR spectra of solvent-free mixtures of **1** with pyridine is very similar to that in IR spectra of solutions in FC-72.[12] The advantage of the solvent-free mixtures is that the concentrations are higher and thus the absorbances are higher than are achievable in solution. Doan has noted that perfluoropolyethers, such as **1**, are in themselves a fluorous anhydrous fluid medium;[22] therefore, pairwise functional group interactions can be studied in a "solvent-free" environment to obtain spectra with higher signal-to-noise ratios. In principle, absorbances can be increased by increasing path length; however, the solvent background is significant. We have found that 1 mm is the longest path length that we can use and still derive information in the carboxylate region of the spectrum. Another difficulty in interpreting the spectra arises with quinoline and isoquinoline. Complexes from a titration of quinoline with **1** give IR spectra with overlapping carboxylic acid carboxylate bands and quinolinium bands. Thus, we have used second derivative spectroscopy to accentuate band profiles for sharp peaks and reveal small shoulders, allowing overlapped peaks to be identified.[51]

The results of a solvent-free titration of neat quinoline with **1** are shown in Figure 8; spectra not required for understanding the system have been removed for graphical clarity, and the entire data set can be found in the Supporting Information (Figure S16). A similar titration of **1** with quinoline in FC-72 was performed to ensure that the solvent-free fluorous environment is representative of a fluorous solvent. The resulting spectra are shown in the Supporting Information (Figure S17). The solvent background in the region below 1675 cm^{-1} gives rise to significant noise in this region of the spectra. The quinoline ring region of the second-order derivative spectra is shown in Figure 9. The peak positions and assignments are summarized in Table 3.

Let us first discuss the quinoline ring region of the spectra (∼1650−1400 cm^{-1}). We observe four strong bands at 1621, 1597, 1571, and 1501 cm^{-1} for quinoline. These observations are consistent with the observations of Dines.[52] In the titration of quinoline (B) with **1** (HA) (Figures 8 and 9), molar ratios below 1:2 exhibit bands at 1503 and 1602 cm^{-1} that can be attributed to ring vibrations of hydrogen-bonded quinoline (B·HA) in accordance with Dines et al.[52] Figure 9 shows that, as additional **1** is added, these bands are replaced with bands at 1638, 1604, 1567, and 1490 cm^{-1} that can be assigned to quinolinium (BH^+) vibrations. The band at 1638 cm^{-1} is broad[52] and thus does not appear strong in the second derivative spectrum (Figure 9), but it is easily seen as a shoulder in Figure 8. In support of the assignments for the quinolinium ion, Dines[52] observed bands at 1638, 1597, 1559, and 1489 cm^{-1} for quinolinium adsorbed on silica. Those bands were assigned to quinolinium based on calculations (bands predicted at 1634, 1594, 1583, 1551, and 1467 cm^{-1}).

Moving to the carbonyl region of the spectra, **1** (black line, Figures 7 and S17) exhibits a vibration centered at 1775 cm^{-1} that is characteristic of the carboxylic acid carbonyl stretch of the cyclic **1**-dimer (HA_2).[22] In Figure 8, the broad band near 1697 cm^{-1} is assigned to the ionic complex. Additional **1** causes a shift in this band from 1697 cm^{-1} to lower energy. These bands can be assigned to the carboxylate stretch (A^-) of the ionic complex. The wavenumber shift that is observed is caused by "solvation" of the ionic complex by additional acids. It is proposed that these "solvating" acid molecules are necessary to stabilize the hydrogen bond to facilitate the sequential

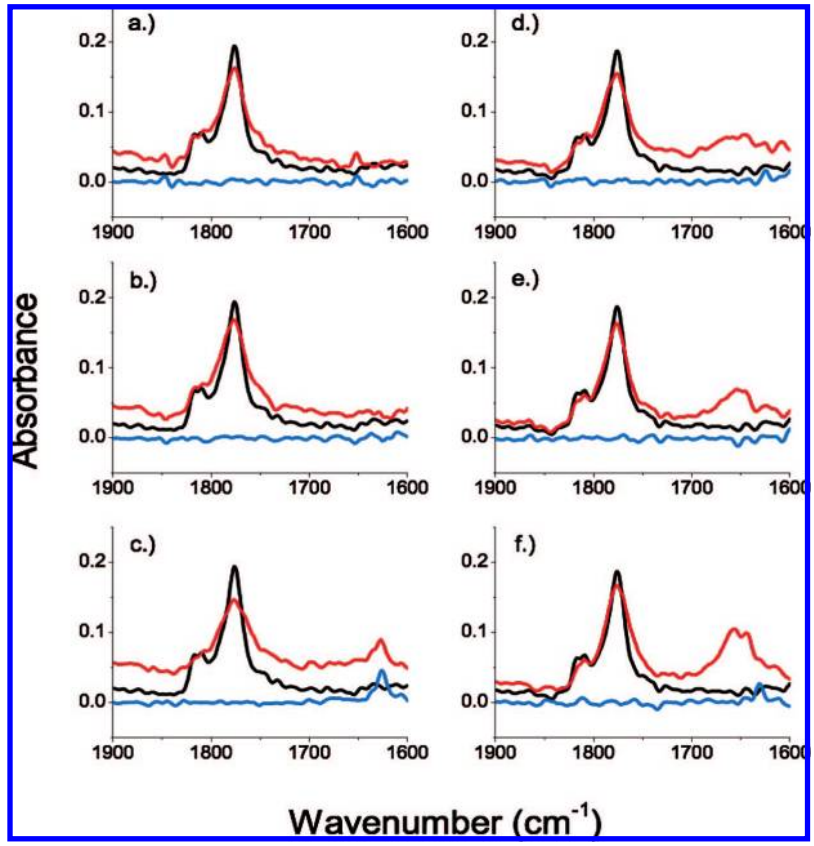

Figure 7. The carbonyl region of representative IR spectra from titration experiments. The colored lines represent **1** (black), base (blue), and the base/**1** complex (red) for (a) pyrazine, (b) pyrimidine, (c) quinazoline, (d) quinoline, (e) pyridine, and (f) isoquinoline, respectively. The spectra on the left (a−c) form 1:1 molecular complexes, whereas the spectra on the right (d−f) form 1:3 (base/acid) ionic complexes.

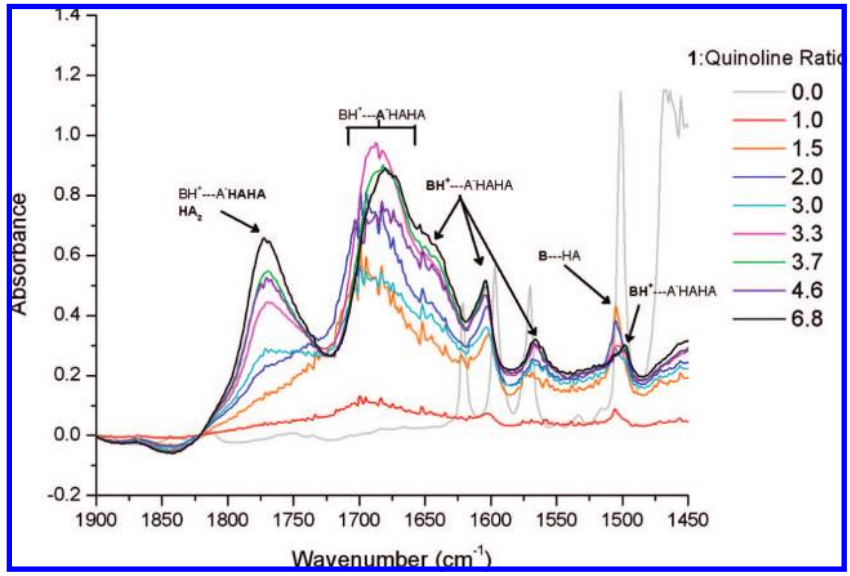

Figure 8. Representative spectra from a solvent-free FTIR titration of constant quinoline with **1**. B, quinoline; HA, I; B−HA; quinoline/**1** molecular complex; BH^+−A^-HAHA, quinolinium/**1**/carboxylate ionic complex. The portion of the complex shown in bold is responsible for the vibration.

formation of a 1:3 quinoline/**1** ionic complex from a 1:1 molecular complex in a nonpolarizable, poorly solvating fluorous environment. The carbonyl (HA) bands (near 1775 cm^{-1}) of acids that are associated with quinoline but not directly hydrogen-bonded to the heterocyclic nitrogen (i.e., "solvating" acids) become significant above ratios of 1:2 (quinoline/**1**). With excess acid, the result is a single broadened band spanning 1725−1625 cm^{-1} that is clearly two overlapping peaks, one from the carboxylate carbonyl and one from quinolinium. Crystalline perfluorodecanoic acid−quinoline also produced an IR spectrum (Figure S18 in the Supporting Information) containing a convoluted carboxylate/quinolinium band spanning 1800−1600 cm^{-1} with sharp quinolinium (BH^+) ring vibrations (1638 cm^{-1}) and hydrogen-bonded quinoline bands (1602 cm^{-1}).

3.3. Solvent Effects. Figure 10 displays data from the literature on complexes between N-heterocyclic bases and carboxylic acids in a range of solvents. Results from the current work are included. The axes correspond to the Kamlet−Taft

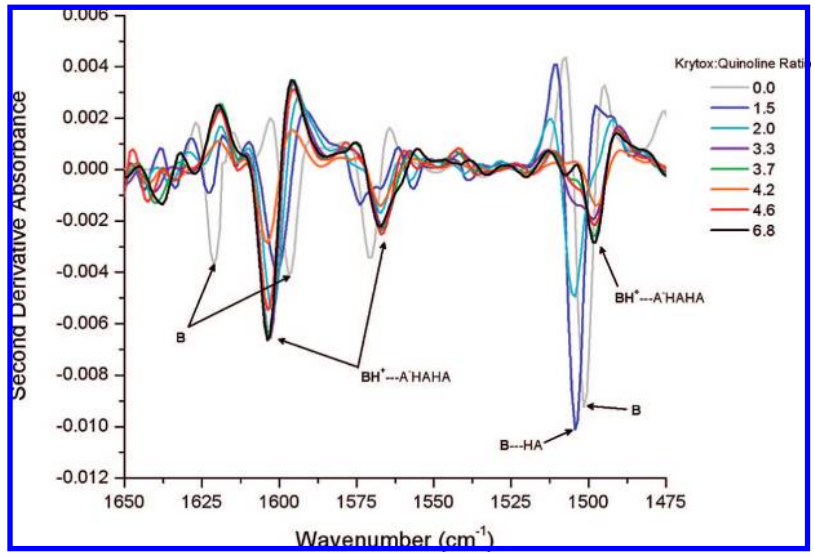

Figure 9. The quinoline-ring region from representative second-derivative IR spectra resulting from a solvent-free titration of neat quinoline with **1**. B, quinoline; HA, **1**; B—HA; quinoline/**1** molecular complex; BH^+—A^-HAHA, quinolinium/**1**/carboxylate ionic complex. The portion of the complex shown in bold is responsible for the vibration.

TABLE 3: Observed Frequencies of the Second Derivative IR Bands in the Carbonyl and Quinoline Ring Vibrational Regions Resulting from a Solvent-free Titration of Quinoline with 1 along with the Peak Assignments[a]

compound	band (cm^{-1})	assignment	description
1 (HA)	1817	C═O	monomer
	1808	C═O	polymer
	1775	C═O	dimer
quinoline (B)	1621	ring	free
	1597	ring	free
	1571	ring	free
	1501	ring	free
	1468	ring	free
(1:1) B:HA	1601	ring	**B**·HA
	1503	ring	**B**·HA
(1:1) B:HA	1638	ring	**BH^+**·A^-
	1604	ring	**BH^+**·A^-
	1567	ring	**BH^+**·A^-
	1490	ring	**BH^+**·A^-
(1:2) B:HA	1680	COO^-	BH^+·**A^-**·HA
	1670	COO^-	BH^+·**A^-**·HA
(1:3) B:HA	1777	C═O	BH^+·A^-·**HA**·HA; **HA_2**
	1767	C═O	BH^+·A^-·HA·**HA**
	1697	COO^-	BH^+·**A^-**·HA·HA

[a] B, quinoline; BH^+, quinolinium; HA, **1**-acid; A^-, **1**-carboxylate. The portion of the complex shown in bold is responsible for the vibration.

dipolarity/polarizability parameter (π^*)[53] of the solvent and the difference between the proton donating power of the conjugate acid of the base in water (pK_{aBH^+}) and that of the acid (pK_{aHA}) also in water.

$$\Delta pK_a = pK_{aBH^+} - pK_{aHA} \quad (2)$$

Each data point represents a hydrogen-bonded complex between an acid, HA, and a base, B. Squares represent molecular complexes (B—HA), and circles represent ionic complexes (BH^+—A^-). Large symbols are data reported here, and the smaller symbols represent data in the literature (see Table S1 and S2 in the Supporting Information for the citations). Note that the current work is mainly focused on the lower right side of the graph where there was a paucity of data. The stoichiometry of each complex, if known, is indicated by the color of the point (see legend). This graphical view is necessarily approximate. The temperature and concentrations used vary among the reported data, the use of pK_a values measured in water for processes occurring in other solvents must be to some degree inaccurate, and π^* by itself is insufficient to explain the effect of a solvent on acid, base, or complex free energy. With these caveats in mind, though, there is still information to be gained from Figure 10.

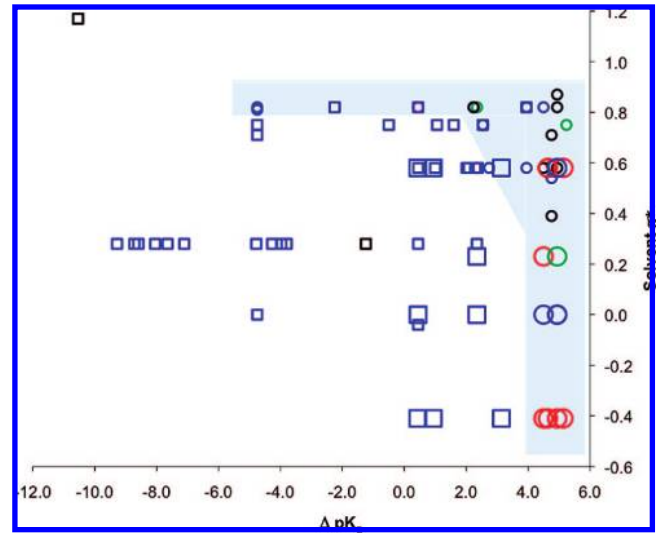

Figure 10. A survey of complexation between N-heterocyclic bases with carboxylic acids in a variety of solvents. Squares and circles represent molecular and ionic complexes, respectively; small symbols (○,□) are literature data and large symbols (○,□) are data reported here. 1:1 complexes are shown in blue, 1:2 (base:acid) in green, and 1:3 in red. Complexes with unknown stoichiometry are shown in black. The shaded zone is where proton transfer has been observed. See the Supporting Information for the data table. $\Delta pK_a = pK_{aBH^+} - pK_{aAH}$; π^* = Kamlet—Taft dipolarity/polarizability parameter.

We note that there are two areas where circles (ionic complexes) are found, in polar solvents (top) and when ΔpK_a is large (right). Pyridinium (aqueous $pK_a = 5.2$) is observed with acids as weak as 4-fluorophenol, if the solvent is sufficiently polar, as well as in highly nonpolar fluorous solvents, if the acid has a sufficiently low pK_a. Pyridinium—carboxylate com-

TABLE 4: Occurance of Proton Transfer in the Complexation between Trifluoroacetic Acid (Organic Solvents) or 1 (FC-72) and Isoquinoline in Increasingly Polar Solvents

solvent	π^*	stoichiometry (B:HA)	type
acetonitrile[48]	0.75	1:1	$BH^+ \cdot A^-$
chlorobenzene[48]	0.71	1:1	$BH^+ \cdot A^-$
benzene[48]	0.59	1:1	$B \cdot HA/BH^+ \cdot A^-$
chloroform[a48,54]	0.58	1:1/1:2 mixture	$B \cdot HA/BH^+ \cdot A^- \cdot HA$
toluene[48]	0.54	1:1/1:2 mixture	$B \cdot HA/BH^+ \cdot A^- \cdot HA$
butyl chloride[48]	0.39	1:1/1:2 mixture	$B \cdot HA/BH^+ \cdot A^- \cdot HA$
carbon tetrachloride[48]	0.28	1:1/1:2 mixture	$B \cdot HA/BH^+ \cdot A^- \cdot HA$
FC-72	−0.41	1:3	$BH^+ \cdot A^- \cdot HA \cdot HA$

[a] The 1:2 ionic form is dominant under conditions of excess acid.

plexes in more polar solvents, such as dichloromethane and tetrachloroethylene,[36] are 1:1, whereas ionic complexes observed in lower polarity solvents, including fluorous solvents, often have more complex stoichiometries.

Isoquinoline−trifluoroacetic acid complexes in a range of solvents (hexane, octane, carbon tetrachloride, toluene, butyl chloride, chloroform, acetonitrile,[48] and FC-72) are included in Figure 10 and are summarized in Table 4. The data show that the 1:1 complex changes from molecular to ionic with increasing solvent polarity.[48] It was reported that the electronic spectra of the ionic 1:2 complexes were not sensitive to the solvent. Through continuous variations experiments and IR spectroscopy (Figures 1 and 7), we have observed a 1:3 isoquinoline/**1** ionic complex in FC-72, thereby confirming that more complex stoichiometry is required for proton transfer in fluorous solvents.

It is clear from the data that excess acid is generally required for proton transfer to occur in nonpolar environments. Fluorous solvents require a larger excess of acid to base, 3:1, compared to the 2:1 excess observed in nonpolar organic solvents. Reversible proton transfer along the N—H—O hydrogen bridge in a fluorous environment can be schematically represented by the following equations,

$$(HA)_2 \rightleftharpoons 2HA \quad \text{(a)}$$

$$B + HA \rightleftharpoons B \cdot HA \quad \text{(b)}$$

$$(B \cdot HA) + nHA \rightleftharpoons (BH^+ \cdot A^-)(HA)_n \quad \text{(c)}$$

where B is a pyridine-like base and HA is a fluorous-soluble acid. The hydrogen bonds of the carboxylic acid dimer[12] must first be broken (eq a), followed by formation of a base-acid hydrogen-bonded complex (eq b). In nonpolarizable environments such as fluorous liquids, solvation by additional acids (eq c) is necessary to facilitate proton transfer. Of the bases listed in Table 1, only those that formed 1:3 (base/acid) complexes with **1** in FC-72 (quinoline, pyridine, and isoquinoline), show evidence of proton transfer (large red circles in Figure 10). The complexes of pyrazine, pyrimidine, and quinazoline are molecular and 1:1 (large blue squares in Figure 10). Proton transfer and the concurrent rearrangement of acid molecules, or rearrangement of the solvent in polar environments, are accompanied by a significant decrease in entropy. Therefore, for proton transfer to be energetically favorable, the free energy of formation of the complex must compensate for the entropic costs of forming a higher-order complex.

4. Conclusions

We have shown that proton transfer and stabilization of the cationic BH^+ occurs in strongly polar solvents and occurs in nonpolar fluorous solvents, but only with excess acid. Although a 2-fold excess of acid is sufficient to promote proton transfer in nonpolar organic solvents, a 3-fold excess is necessary in fluorous solvents. 1:3 ionic hydrogen bonds ($BH^+ \cdot A^-HAHA$) are observed in complexes of quinoline, isoquinoline, and pyridine with **1** in FC-72. Proton transfer is possible in such a nonpolar environment because the additional acids solvate the ionic bond and shield it from the environment. The stoichiometry and formation of ionic complexes have been demonstrated using continuous variations methods and IR spectroscopy. 1:1 molecular complexes ($B \cdot HA$) were observed between pyrazine, pyrimidine, and quinazoline and **1** in FC-72. We suggested that the free energy of complex formation between these bases and **1** is not enough to compensate for the free energy cost of the acid dimer dissociation and ordering required to solvate the ionic bond. Forcing the higher-order complexes by employing such a nonpolar solvent could also prove useful in supramolecular chemistry applications.

Acknowledgment. This research was funded by the National Science Foundation (NSF) through grants CHE 0315188 and CHE 0615952.

Supporting Information Available: A derivation of the normalized method of continuous variations, figures (S1) showing a continuous variations plot for a quinoline−$\mathbf{1}_2$ complex in FC-72; (S2) UV spectra from a constant-volume titration of pyrimidine with **1** in FC-72; (S3) titration curve at 236 nm from a titration of pyrimidine with **1** in FC-72; (S4) UV spectra from a constant-volume titration of pyrazine with **1** in FC-72; (S5) titration curve at 261 nm from a titration of pyrazine with **1** in FC-72; (S6) UV spectra from a constant-volume titration of quinazoline with **1** in FC-72; (S7) titration curve at 224 nm from a titration of quinazoline with **1** in FC-72; (S8) UV spectra from a constant-volume titration of pyridine with **1** in FC-72; (S9) titration curve at 255 nm from a titration of pyridine with **1** in FC-72; (S10) UV spectra from a constant-volume titration of isoquinoline with **1** in FC-72; (S11) titration curvesat 320 and 327 nm from a titration of isoquinoline with **1** in FC-72; (S12) Position of the $\pi \rightarrow \pi^*$ electronic absorption band of a isoquinoline−**1** complex as a function of **1**/isoquinoline ratio in a constant-volume titration of isoquinoline with **1** in FC-72; (S13) UV spectra from a constant-volume titration of quinoline with **1** in FC-72; (S14) titration curve at 314 nm resulting from a titration of quinoline with **1** in FC-72; (S15) overlay of predicted concentration profiles from model-free EFA and regression analysis of the UV spectra resulting from a constant-volume titration of isoquinoline with **1** in FC-72; (S16) IR spectra showing carbonyl and quinoline ring vibrational regions from a solvent-free titration of neat quinoline with **1**; (S17) IR spectra showing carbonyl and quinoline ring vibrational regions from a titration of constant 2.5 mM **1** with quinoline in FC-72; (S18) IR spectrum of a perfluorodecanoic acid-quinoline crystal/KBr pellet; (Table S1) a listing of literature and experimental data corresponding to molecular complexes shown in Figure 10; and (Table S2) a listing of literature and experimental data corresponding to ionic complexes shown in Figure 10. This information is available free of charge via the Internet at http://pubs.acs.org.

References and Notes

(1) Lehn, J.-M. *Macrocyclic Chemistry − Aspects of Organic and Inorganic Supramolecular Chemistry*; Wiley-VCH: Weinheim, 1993.

(2) Schrader, T.; Hamilton, A. D. *Functional Synthetic Receptors*; Wiley-VCH: Weinhelm, 2005.

(3) Ansyln, E. V.; Dougherty, D. A. *Modern Physical Organic Chemistry*; University Science Books: Sausalito, CA, 2006.
(4) Valenta, J. N.; Dixon, R. P.; Hamilton, A. D.; Weber, S. G. *Anal. Chem.* **1994**, *66*, 2397.
(5) Buhlmann, P.; Badertscher, M.; Simon, W. *Tetrahedron* **1993**, *49*, 595.
(6) Shinkai, S.; Tsukagoshi, K.; Ishikawa, Y.; Kunitake, T. *J. Chem. Soc., Chem. Comm.* **1991**, 1039.
(7) Shoji, Y.; Tashiro, K.; Aida, T. *J. Am. Chem. Soc.* **2004**, *126*, 6570.
(8) Oshima, T.; Higuchi, H.; Ohto, K.; Inoue, K.; Goto, M. *Langmuir* **2005**, *21*, 7280.
(9) Lipkowitz, K. B.; Raghothama, S.; Yang, J. A. *J. Am. Chem. Soc.* **1992**, *114*, 1554.
(10) Hunter, C. A. *Angew. Chem., Int. Ed.* **2004**, *43*, 5310.
(11) Li, S.; Sun, L.; Chung, Y.; Weber, S. G. *Anal. Chem.* **1999**, *71*, 2146.
(12) O'Neal, K.; Geib, S.; Weber, S. G. *Anal. Chem.* **2007**, *79*, 3117.
(13) Gladysz, J. A.; Curran, D. P.; Horvath, I. T. *Handbook of Fluorous Chemistry*; Wiley-VCH: Weinheim, Germany, 2004.
(14) Horvath, I. T.; Rabai, J. *Science* **1994**, *266*, 72.
(15) Curran, D. P.; Lee, Z. *Green Chem.* **2001**, *3*, G3.
(16) Vincent, J.-M. *J. Fluorine Chem.* **2008**, In Press, Corrected Proof.
(17) Vincent, J.-M.; Contel, M.; Laguna, M.; Fish, R. H. $Mn_2^+/Co_2^+/Cu_2^+/Cu^+$ complexes of fluoroponytailed R_f-tris-N-1,4,7-triazacyclononane and R_f-carboxylate, $C_8F_{17}(CH_2)_2COOH$. Precatalysts for FBC alkane, alkene, and alcohol oxidation chemistry. In *Handbook of Fluorous Chemistry*; Weinheim: Germany, 2004; pp 395.
(18) Hope, E. G.; Kemmitt, R. D. W.; Stuart, A. M. *J. Am. Chem. Soc., Dalt. Trans.* **1998**, 3765.
(19) Bakkari, M. E.; McClenaghan, N.; Vincent, J.-M. *J. Am. Chem. Soc.* **2002**, *124*, 12942.
(20) Bakkari, M. E.; Vincent, J.-M. *Org. Lett.* **2004**, *6*, 2765.
(21) Boswell, P. G.; Buhlmann, P. *J. Am. Chem. Soc.* **2005**, *127*, 8958.
(22) Doan, V.; Koppe, R.; Kasai, P. H. *J. Am. Chem. Soc.* **1997**, *119*, 9810.
(23) Boenigk, D.; Mootz, D. *J. Am. Chem. Soc.* **1988**, *110*, 2135.
(24) Golubev, N. S.; Smirnov, S. N.; Gindin, V. A.; Denisov, G. S.; Benedict, H.; Limbach, H.-H. *J. Am. Chem. Soc.* **1994**, *116*, 12055.
(25) Barrow, G. M. *J. Am. Chem. Soc.* **1956**, *78*, 5802.
(26) Odinokov, S. E.; Mashkovsky, A. A.; Glazunov, V. P. *Spectrochim. Acta* **1976**, *32A*, 1355.
(27) Dawa, B. A.; Gowland, J. A. *Can. J. Chem.* **1978**, *56*, 2567.
(28) Kasende, O.; Zeegers-Huyskens, T. *J. Phys. Chem.* **1984**, *88*, 2132.
(29) Denisov, G. S.; Gindin, V. A.; Golubev, N. S.; Ligay, S. S.; Shchepkin, D. N.; Smirnov, S. N. *J. Mol. Liq.* **1995**, *67*, 217.
(30) Langner, R.; Zundel, G. *J. Am. Chem. Soc., Far. Trans.* **1995**, *91*, 3831.
(31) Golubev, N. S.; Denisov, G. S.; Smirnov, S. N.; Shchepkin, D. N. *Z. Physik. Chem.* **1996**, *196*, 73.
(32) Drichko, N. V.; Kerenskaia, G. Y.; Schreiber, V. M. *J. Mol. Struct.* **1999**, *477*, 127.
(33) Magonski, J. *J. Phys. Org. Chem.* **2002**, *15*, 204.
(34) Berg, E. R.; Freeman, S. A.; Green, D. D.; Ulness, D. J. *J. Phys. Chem.* **2006**, *110*, 13434.
(35) Berg, E. R.; Green, D. D.; Moliva, A, D. C.; Bjerke, B. T.; Gealy, M. W.; Ulness, D. J. *J. Phys. Chem., A* **2008**, *112*, 833.
(36) Joris, L.; Mitsky, J.; Taft, R. W. *J. Am. Chem. Soc.* **1972**, *94*, 3438.
(37) Denisov, G. S.; Kulbida, A. I.; Micheev, V. A.; Rumynskaja, I. G.; Schreiber, V. M. *J. Mol. Liq.* **1983**, *26*, 159.
(38) Jeffrey, G. A. *An Introduction to Hydrogen Bonding*; Oxford University Press: New York, 1997.
(39) Job, A. *Ann. Chim. (Paris, Fr.)* **1928**, *9*, 113.
(40) Connors, K. A. *Binding Constants*, 411 ed.; John Wiley & Sons: New York, 1987.
(41) Likussar, W.; Boltz, D. F. *Anal. Chem.* **1971**, *43*, 1265.
(42) Binstead, R. A.; Jung, B.; Zuberbuhle, A. D. *SPECFIT/32TM Global Analysis System*, 3.0 ed.; Spectrum Software Associates, 2004.
(43) Momoki, K.; Sekino, J.; Sato, H.; Yamaguchi, N. *Anal. Chem.* **1969**, *41*, 1286.
(44) Peral, F.; Gallego, E. *J. Mol. Struct.* **1995**, *372*, 101.
(45) Peral, F.; Gallego, E. *Spectrochimica Acta Part A* **2003**, *59*, 1223.
(46) Albert, A.; Armarego, W. L. F.; Spinner, E. *J. Chem. Soc.* **1961**, 2689.
(47) Peral, F.; Gallego, E. *J. Mol. Struct.* **1994**, *326*, 59.
(48) Denisov, G. S.; Mikheev, V. A.; Sorkornov, A. B.; Sorkornov, T. V.; Terushkin, B. S.; Shraiber, V. M. *Zh. Prikl. Spektrosk.* **1985**, 66.
(49) Harris, D. C.; Bertolucci, M. D. *Symmetry and Spectroscopy: An Introduction to Vibrational and Electronic Spectroscopy*; Dover Publications: New York, NY, 1978.
(50) Bulmer, J. T.; Shurvell, H. F. *J. Phys. Chem.* **1973**, *77*, 256.
(51) Dega-Szafran, Z.; Grundwald-Wyspianska, M.; Szafran, M. *Spectrochimica Acta, Part A* **1991**, *47*, 543.
(52) Dines, T. J.; MacGregor, L. D.; Rochester, C. H. *Langmuir* **2002**, *18*, 2300.
(53) Kamlet, M. J.; Abboud, J. L.; Taft, R. W. *J. Am. Chem. Soc.* **1977**, *99*, 6027.
(54) Sokornova, T. V.; Shraiber, V. M. *Zh. Prikl. Spektrosk.* **1992**, *56*, 200.

JP8084155